arXiv:1604.04709v1 [hep-ph] 16 Apr 2016

Heavy Pseudoscalar Twist-3 Distribution Amplitudes within QCD Theory in Background Fields

Tao Zhong[1],* Xing-Gang Wu[2],† Tao Huang[3],‡ and Hai-Bing Fu[4]§
[1] *Department of Physics, Henan Normal University, Xinxiang 453007, P.R. China*
[2] *Department of Physics, Chongqing University, Chongqing 401331, P.R. China*
[3] *Institute of High Energy Physics and Theoretical Physics Center for Science Facilities, Chinese Academy of Sciences, Beijing 100049, P.R. China*
[4] *School of Science, Guizhou Minzu University, Guiyang 550025, P. R. China*
(Dated: April 19, 2016)

In this paper, we study the properties of the twist-3 distribution amplitude (DA) of the heavy pseudo-scalars such as η_c, B_c and η_b. New sum rules for the twist-3 DA moments $\langle\xi_P^n\rangle_{\rm HP}$ and $\langle\xi_\sigma^n\rangle_{\rm HP}$ up to sixth orders and up to dimension-six condensates are deduced under the framework of the background field theory. Based on the sum rules for the twist-3 DA moments, we construct a new model for the two twist-3 DAs of the heavy pseudo-scalar with the help of the Brodsky-Huang-Lepage prescription. Furthermore, we apply them to the $B_c \to \eta_c$ transition form factor ($f_+^{B_c\to\eta_c}(q^2)$) within the light-cone sum rules approach, and the results are comparable with other approaches. It has been found that the twist-3 DAs $\phi_{3;\eta_c}^P$ and $\phi_{3;\eta_c}^\sigma$ are important for a reliable prediction of $f_+^{B_c\to\eta_c}(q^2)$. For example, at the maximum recoil region, we have $f_+^{B_c\to\eta_c}(0) = 0.674 \pm 0.066$, in which those two twist-3 terms provide $\sim 33\%$ and $\sim 22\%$ contributions. Also we calculate the branching ratio of the semi-leptonic decay $B_c \to \eta_c l\nu$ as $Br(B_c \to \eta_c l\nu) = \left(9.31^{+2.27}_{-2.01}\right) \times 10^{-3}$.

PACS numbers: 11.55.Hx, 14.40.-n

I. INTRODUCTION

The heavy pseudo-scalar (HP), such as B_c, η_c or η_b, is a ground-state meson constituted by a heavy quark and an anti-quark. For exclusive process involving the HP, its distribution amplitude (DA) is usually key component for predicting the decay widths or the production cross-sections of those processes. Thus a more precise HP DA shall lead to a more precise predictions.

Due to non-relativistic nature of the heavy constituent quark/antiquark, the leading-twist DA (or the twist-2 DA) of the HP can be roughly treated as a δ-function [1], i.e. in the leading order of the expansion over the relative velocities, the quark and the antiquark in the HP DA simply share the momentum of the meson according to their masses. For examples, the asymptotic DA of the charmonium and the bottomonium are $\phi_{2;\rm HP}^{\rm asy}(x) \sim \delta(x-1/2)$. By taking the relativistic effect, the heavy-quark mass effect and/or the three-particle effect into account, such a simple asymptotic DA shall be broadened to a certain degree, cf. Refs.[1–3]. Several models for a broader and more realistic HP twist-2 DA have been suggested in the literature, such as the Bondar-Chernyak (BC) model [4], the Bodwin-Kang-Lee (BKL) model [5], the Ma-Si (MS) model [6], the Braguta-Likhoded-Luchinsky (BLL) model [7], the model with the Brodsky-Huang-Lepage (BHL) prescription [8, 9], and etc. A comparison of various η_c twist-2 DA has been done in Ref.[10], in which it has also pointed out that by using a proper η_c twist-2 DA, one may resolve the disagreement between the experimental observations and the NRQCD prediction on the production cross-section of $e^+e^- \to J/\Psi + \eta_c$.

The background field theory (BFT) [11–13] provides a systematic approach for achieving the goal of SVZ sum rules [14] and also provides a physical picture for the vacuum condensates. In Ref. [15], by using the SVZ sum rules within the framework of BFT, we have made a detailed study on the properties of the HP twist-2 DA and have constructed a new model for the twist-2 DA. According to our knowledge on the pionic cases, in addition to the twist-2 DA, the high-twist DA may also provide sizable contributions to the HP-involved processes, even though they are generally power suppressed. Taking the $B \to \pi$ transition form factor (TFF) as an example, a large contribution from the pion twist-3 DAs $\phi_{3;\pi}^P$ and $\phi_{3;\pi}^\sigma$ in comparison to its twist-2 DA has been observed in both the intermediate and the large Q^2-region [16–19]. It is thus interesting to have a reliable way to estimate the properties of the HP twsit-3 DA, which may also have sizable contributions to high-energy processes but are less known so far.

In the present paper, as a step forward, we shall study the HP twist-3 DAs $\phi_{3;\rm HP}^P$ and $\phi_{3;\rm HP}^\sigma$ by using the same approach of Ref.[15]. We shall first estimate the moments of $\phi_{3;\rm HP}^P$ and $\phi_{3;\rm HP}^\sigma$ up to dimension-six by using the SVZ sum rules within the framework of BFT. Then, we shall construct a model for $\phi_{3;\rm HP}^P$ and $\phi_{3;\rm HP}^\sigma$ with the help of the BHL-prescription. In this way the HP twist-3 DAs with a better end-point behavior can be achieved. Finally, as an application of the constructed HP twist-3 DAs, we shall apply them to the $B \to \eta_c$

*Electronic address: zhongtao@htu.edu.cn
†Electronic address: wuxg@cqu.edu.cn
‡Electronic address: huangtao@ihep.ac.cn
§Electronic address: fuhb@cqu.edu.cn

TFF $f_+^{B_c\to\eta_c}(q^2)$.

The remaining parts of the paper are organized as follows. In Sec.II, we construct a light-cone harmonic oscillator model for the HP twist-3 DA with the help of the BHL-prescription. The DA moments are calculated with SVZ sum rules within the framework of BFT. The corresponding numerical results are presented in Sec.III. As an application of the suggested HP twist-3 DA model, we give the light-cone sum rules (LCSR) for $f_+^{B_c\to\eta_c}(q^2)$ by using the conventional correlator, and a comparison of $f_+^{B_c\to\eta_c}(q^2)$ with other approaches are also given in Sec.IV. Finally,Sec.V is reserved for a summary.

II. CALCULATION TECHNIQUE

A. Model for the HP Twist-3 DA

Based on the BHL-prescription [20], a light-cone harmonic oscillator model for the HP twist-2 wave function (WF) has been built in Ref. [15] [1]. After integrating out the transverse momentum $\mathbf{k}_\perp$ component of the WF, the corresponding DA is achieved. Similarly, the HP twist-3 DA $\phi^P_{3;\rm HP}$ can be constructed as

$$\begin{aligned}\phi^P_{3;\rm HP}(x,\mu_0) &= \frac{\sqrt{6}A^P_{\rm HP}(\beta^P_{\rm HP})^2}{\pi^2 f_{\rm HP}}x(1-x)\varphi^P_{\rm HP}(x)\\ &\times \exp\left[-\frac{\hat{m}_1^2(1-x)+\hat{m}_2^2 x}{8(\beta^P_{\rm HP})^2x(1-x)}\right]\\ &\times \left(1-\exp\left[-\frac{\mu_0^2}{8(\beta^P_{\rm HP})^2x(1-x)}\right]\right),\end{aligned} \tag{1}$$

where $f_{\rm HP}$ stands for the HP decay constant, $\hat{m}_{1,2}$ are constituent quark masses of the HP, μ_0 is the factorization scale, and $\mathrm{Erf}(x)=\frac{2}{\sqrt{\pi}}\int_0^x e^{-t^2}dt$ is the error function. The constituent quark masses $\hat{m}_1=\hat{m}_b$ and $\hat{m}_2=\hat{m}_c$ for the case of B_c-meson and $\hat{m}_1=\hat{m}_2=\hat{m}_c(\hat{m}_b)$ for the case of $\eta_c(\eta_b)$-meson. We take $\hat{m}_c=1.8$GeV and $\hat{m}_b=4.7$GeV to do our numerical calculation. $A^P_{\rm HP}$ is the normalization constant. The harmonious parameter $\beta^P_{\rm HP}$ dominantly determines the transverse distribution of the DA. The function $\varphi^P_{\rm HP}(x)$ dominates the DA longitudinal distribution, which is expressed by a Gegenbauer polynomial. Keeping its first several terms, we have

$$\varphi^P_{\rm HP}(x)=1+\sum_{n=1}^{6}B_n^{{\rm HP},P}\times C_n^{1/2}(2x-1). \tag{2}$$

Due to the same mass for the heavy constituent quark and anti-quark, the twist-3 DA $\phi^P_{3;\eta_c}$ and $\phi^P_{3;\eta_b}$ of η_c and η_b mesons are symmetric under the transformation of $x\leftrightarrow(1-x)$, thus we have $B^{\eta_c,P}_{2m-1}=B^{\eta_b,P}_{2m-1}=0$ for $(m\geq 1)$.

The input parameters $A^P_{\rm HP}$, $B_n^{{\rm HP},P}$ and $\beta^P_{\rm HP}$ are determined by the following constraints:

- The normalization condition of $\phi^P_{3;\rm HP}$,

$$\int_0^1 dx\phi^P_{3;\rm HP}(x,\mu_0)=1. \tag{3}$$

- The average value of the squared HP transverse momentum $\langle\mathbf{k}_\perp^2\rangle_{\rm HP}$, which is defined as

$$\begin{aligned}\langle\mathbf{k}_\perp^2\rangle_{\rm HP} &= \frac{(A^P_{\rm HP})^2(\beta^P_{\rm HP})^4}{\pi^2 P_{\rm HP}}\int_0^1 dx x^2(1-x)^2\\ &\times (\varphi^P_{\rm HP}(x))^2\exp\left[-\frac{\hat{m}_1^2(1-x)+\hat{m}_2^2x}{4(\beta^P_{\rm HP})^2x(1-x)}\right],\end{aligned} \tag{4}$$

  where $P_{\rm HP}$ stands for the probability of finding the valence quark state $|Q_1\bar{Q}_2\rangle$ in the HP Fock-state expansion, and we take, $P_{\eta_c}\simeq 0.8$ and $P_{B_c}\sim P_{\eta_b}\simeq 1$ [15]. At present, there is no definite value for $\langle\mathbf{k}_\perp^2\rangle_{\rm HP}$, and we predict its value via a comparison of the cases of the pion and the B/D mesons that are better known. The average values of the squared transverse momentum of D and B mesons are sensitive to their decay constants f_D and f_B [22], $\langle\mathbf{k}_\perp^2\rangle^{1/2}_{D(B)}\propto f_{D(B)}$. It is reasonable to assume that this is also satisfied by the HP meson, $\langle\mathbf{k}_\perp^2\rangle^{1/2}_{\rm HP}\propto f_{\rm HP}$. Moreover, we connect the HP value $\langle\mathbf{k}_\perp^2\rangle^{1/2}_{\rm HP}$ to the case of pion (the light pseudoscalar) as, $\langle\mathbf{k}_\perp^2\rangle^{1/2}_{\rm HP}/f_{\rm HP}\simeq\langle\mathbf{k}_\perp^2\rangle^{1/2}_{\pi}/f_\pi$, where $f_\pi=(130.41\pm0.03\pm0.20)$ MeV [23] is the pion decay constant. By further taking $\langle\mathbf{k}_\perp^2\rangle^{1/2}_{\pi}\simeq 350$MeV [22, 24], we finally get $\langle\mathbf{k}_\perp^2\rangle^{1/2}_{\eta_c}\simeq 1.216$ GeV, $\langle\mathbf{k}_\perp^2\rangle^{1/2}_{B_c}\simeq 1.337$ GeV and $\langle\mathbf{k}_\perp^2\rangle^{1/2}_{\eta_b}\simeq 2.177$ GeV. It is noted that the shape of $\phi^P_{3;\rm HP}$ (or $\phi^\sigma_{3;\rm HP}$) is dominated by their moments and is insensitive to the choice of $\langle\mathbf{k}_\perp^2\rangle^{1/2}_{\rm HP}$.

- The twist-3 DA moments $\langle\xi^n_P\rangle_{\rm HP}$ are defined as

$$\langle\xi^n_P\rangle_{\rm HP}|_{\mu_0}=\int_0^1 du(2u-1)^n\phi^P_{3;\rm HP}(u,\mu_0), \tag{5}$$

  which shall be calculated by using the SVZ sum rules within the framework of BFT in the next subsection.

The model of $\phi^\sigma_{3;\rm HP}$ can be constructed via the same way, i.e., by replacing the upper index 'P' with 'σ' in Eqs.(1, 3, 4 and 5), and taking the expansion

$$\varphi^\sigma_{\rm HP}(x)=1+\sum_{n=1}^{6}B_n^{{\rm HP},\sigma}\times C_n^{3/2}(2x-1), \tag{6}$$

[1] For the detail technique, we refer the reader to Ref. [21], where the quark propagator is given with full mass dependence up to dimension-six terms within the framework of BFT.

we can obtain the model for the HP twist-3 DA $\phi^{\sigma}_{3;\rm HP}$.

In the above equations, all the parameters are for the initial scale μ_0, the parameters at any other scale can be obtained via the conventional evolution equation [15, 25].

B. Sum Rules for the Twist-3 DAs $\phi^{P}_{3;\rm HP}$ and $\phi^{\sigma}_{3;\rm HP}$

To derive the sum rules for the moments of the twist-3 DAs $\phi^{P}_{3;\rm HP}$ and $\phi^{\sigma}_{3;\rm HP}$, we adopt the following correlators

$$\begin{aligned}\Pi^{\rm PS}_{\rm HP}(q) &= (z\cdot q)^n I^{\rm PS}_{\rm HP}(q^2)\\ &= i\int d^4x e^{iq\cdot x}\left\langle 0\left|T\left\{J^{\rm PS}_n(x)J^{\rm PS\dagger}_0(0)\right\}\right|0\right\rangle (7)\end{aligned}$$

and

$$\begin{aligned}\Pi^{\rm PT}_{\rm HP}(q) &= -i(q_\mu z_\nu - q_\nu z_\mu)(z\cdot q)^n I^{\rm PT}_{\rm HP}(q)(q^2)\\ &= i\int d^4x e^{iq\cdot x}\left\langle 0\left|T\left\{J^{\rm PT}_n(x)J^{\rm PS\dagger}_0(0)\right\}\right|0\right\rangle (8)\end{aligned}$$

for $\langle\xi^n_P\rangle_{\rm HP}$ and $\langle\xi^n_\sigma\rangle_{\rm HP}$, respectively. Here $z^2=0$, $J^{\rm PS}_n(x)$ and $J^{\rm PT}_n(x)$ stand for the pseudo-scalar and the tensor currents

$$J^{\rm PS}_n(x) = \bar{Q}_1(x)\gamma_5(iz\cdot\overleftrightarrow{D})^n Q_2(x), \quad (9)$$

$$J^{\rm PT}_n(x) = \bar{Q}_1(x)\sigma_{\mu\nu}\gamma_5(iz\cdot\overleftrightarrow{D})^{n+1} Q_2(x) \quad (10)$$

with $Q_1=b$ and $Q_2=c$ for B_c, $Q_1=Q_2=c$ ($Q_1=Q_2=b$) for η_c (η_b), and $\sigma_{\mu\nu}=\frac{i}{2}(\gamma_\mu\gamma_\nu-\gamma_\nu\gamma_\mu)$.

Two correlators (7, 8) can be treated under the standard SVZ sum rules. On the one hand, in the physical region, one can insert a completed set of intermediate hadronic states in the correlators (7, 8). The hadronic transition matrix elements can be written as

$$\begin{aligned}&\left\langle 0\left|\bar{Q}_1(0)\gamma_5(iz\cdot\overleftrightarrow{D})^n Q_2(0)\right|{\rm HP}(q)\right\rangle\\ &\quad = -i\mu_{\rm HP} f_{\rm HP}(z\cdot q)^n\langle\xi^n_P\rangle_{\rm HP}, \quad (11)\\ &\left\langle 0\left|\bar{Q}_1(0)\sigma_{\mu\nu}\gamma_5(iz\cdot\overleftrightarrow{D})^{n+1} Q_2(0)\right|{\rm HP}(q)\right\rangle\\ &\quad = -\frac{n+1}{3}\mu_{\rm HP} f_{\rm HP}\left[1-\frac{(m_1+m_2)^2}{m^2_{\rm HP}}\right]\\ &\quad\times(q_\mu z_\nu - q_\nu z_\mu)(z\cdot q)^n\langle\xi^n_\sigma\rangle_{\rm HP}. \quad (12)\end{aligned}$$

Furthermore, the hadronic spectrum representations can be written as

$$\begin{aligned}{\rm Im}I^{\rm PS}_{\rm HP,had}(s) &= \pi\delta(s-m^2_{\rm HP})\mu^2_{\rm HP}f^2_{\rm HP}\langle\xi^n_P\rangle_{\rm HP}\\ &+ \pi\rho^{\rm had}_P(s)\theta(s-s^P_{\rm HP}), \quad (13)\\ {\rm Im}I^{\rm PT}_{\rm HP,had}(s) &= \pi\delta(s-m^2_{\rm HP})\frac{n+1}{3}\mu^2_{\rm HP}f^2_{\rm HP}\\ &\times\left[1-\frac{(m_1+m_2)^2}{m^2_{\rm HP}}\right]\langle\xi^n_\sigma\rangle_{\rm HP}\\ &+ \pi\rho^{\rm had}_\sigma(s)\theta(s-s^\sigma_{\rm HP}), \quad (14)\end{aligned}$$

where $m_{\rm HP}$ is the HP mass, $\mu_{\rm HP}=\frac{m^2_{\rm HP}}{m_1+m_2}$ with the mass $m_{1(2)}$ of the heavy quark $Q_{1(2)}$. θ stands for the usual step-function and $s^P_{\rm HP}$ and $s^\sigma_{\rm HP}$ indicate the continue threshold parameters. $\rho^{\rm had}_P(s)$ and $\rho^{\rm had}_\sigma(s)$ are hadronic spectrum densities, which can be approximately obtained with the quark-hadron duality [14].

On the other hand, the correlators (7, 8) can be treated by using the operator product expansion (OPE) in the deep Euclidean region. Detailed calculation technique for the OPE under the framework BFT can be found in Ref.[15]. For shortness, we shall not present them here, the interesting reader may turn to Ref.[15] for detail.

By further using the dispersion relation

$$I_{\rm qcd}(q^2)=\frac{1}{\pi}\int^\infty_{t_{\rm min}} ds\frac{{\rm Im}I_{\rm had}(s)}{s-q^2}+{\rm subtractions}, \quad (15)$$

where $t_{\rm min}=(m_1+m_2)^2$, and applying the Borel transformation, we finally obtain the required sum rules for the moments $\langle\xi^n_P\rangle_{\rm HP}$ and $\langle\xi^n_\sigma\rangle_{\rm HP}$,

$$\begin{aligned}&\frac{\mu^2_{\rm HP}f^2_{\rm HP}\langle\xi^n_P\rangle_{\rm HP}}{M^2\exp\left[m^2_{\rm HP}/M^2\right]}\\ &=\frac{1}{\pi}\frac{1}{M^2}\int^{s^P_0}_{t_{min}} ds e^{-s/M^2}{\rm Im}I^{\rm PS}_{\rm HP,pert}(s)+I^{\rm PS}_{\rm HP,\langle G^2\rangle}(M^2)\\ &+I^{\rm PS}_{\rm HP,\langle G^3\rangle}(M^2), \quad (16)\\ &\frac{(n+1)\mu^2_{\rm HP}f^2_{\rm HP}\langle\xi^n_\sigma\rangle_{\rm HP}}{3M^2\exp\left[m^2_{\rm HP}/M^2\right]}\times\left[1-\frac{(m_1+m_2)^2}{m^2_{\rm HP}}\right]\\ &=\frac{1}{\pi}\frac{1}{M^2}\int^{s^\sigma_0}_{t_{min}} ds e^{-s/M^2}{\rm Im}I^{\rm PT}_{\rm HP,pert}(s)+I^{\rm PT}_{\rm HP,\langle G^2\rangle}(M^2)\\ &+I^{\rm PT}_{\rm HP,\langle G^3\rangle}(M^2), \quad (17)\end{aligned}$$

where M stands for the Borel parameter. The functions ${\rm Im}I^{\rm PS,PT}_{\rm HP,pert}(s)$, $I^{\rm PS,PT}_{\rm HP,\langle G^2\rangle}(M^2)$ and $I^{\rm PS,PT}_{\rm HP,\langle G^3\rangle}(M^2)$ stand for imaginary part of the perturbative terms, the contribution proportional to double-gluon condensate $\langle G^2\rangle$ and the contribution proportional to triple-gluon condensate $\langle g^3_s fG^3\rangle$, respectively. For convenience, we put their expressions in the Appendix.

III. THE HP TWIST-3 DAS $\phi^{P}_{3;\rm HP}$ AND $\phi^{\sigma}_{3;\rm HP}$

To do the numerical calculation, we adopt the following Particle Data Group values for the input parameters [23]: $m_{\eta_c}=(2.9837\pm0.0007)$GeV, $m_{B_c}=(6.2745\pm0.0018)$GeV, $m_{\eta_b}=(9.3980\pm0.0032)$GeV; the current quark masses under the $\overline{\rm MS}$-scheme are $\bar{m}_c(\bar{m}_c)=(1.275\pm0.025)$GeV and $\bar{m}_b(\bar{m}_b)=(4.18\pm0.03)$GeV. The one-loop α_s-running is adopted, whose running behavior is fixed by $\alpha_s(m_Z)=0.1185\pm0.0006$ with $m_Z=(91.1876\pm0.0021)$GeV [23]. And we obtain $\Lambda_{\rm QCD}\simeq$ 270MeV, 257MeV and 204MeV for the flavor number $n_f=3$, 4 and 5, respectively. The scale-independence gluon condensates are taken as $\langle\alpha_s G^2\rangle=(0.038\pm0.011)$GeV^4 [14] and $\langle g^3_s fG^3\rangle=(0.013\pm0.007)$GeV^6 [21]. As suggested by Braguta et al. [7], the continuum threshold parameters s^P_0 and s^σ_0 are taken to be infinity, and the

ratio $\langle\xi_P^n\rangle_{\rm HP}/\langle\xi_P^0\rangle_{\rm HP}$ and $\langle\xi_\sigma^n\rangle_{\rm HP}/\langle\xi_\sigma^0\rangle_{\rm HP}$ are adopted to derive the $n_{\rm th}$-moment $\langle\xi_P^n\rangle_{\rm HP}$ and $\langle\xi_\sigma^n\rangle_{\rm HP}$. As for the Borel windows of the sum rules (16, 17), we take $M^2\in[1,2]({\rm GeV}^2)$ for $\langle\xi_P^n\rangle_{\eta_c}$ and $\langle\xi_\sigma^n\rangle_{\eta_c}$, $M^2\in[15,20]({\rm GeV}^2)$ for $\langle\xi_P^n\rangle_{B_c}$, $\langle\xi_\sigma^n\rangle_{B_c}$, $\langle\xi_P^n\rangle_{\eta_b}$ and $\langle\xi_\sigma^n\rangle_{\eta_b}$.

A. Properties of the HP twist-3 DA moments

TABLE I: The HP twist-3 DA moments $\langle\xi_P^n\rangle_{\rm HP}$ up to $6_{\rm th}$-order. The errors are squared average of those from all input parameters, such as the Borel parameter, the condensates and the bound state parameters. The scale μ is set to be $\bar{m}_c(\bar{m}_c)$ for η_c and $\bar{m}_b(\bar{m}_b)$ for B_c and η_b.

	$\eta_c(\bar{m}_c(\bar{m}_c))$	$B_c(\bar{m}_b(\bar{m}_b))$	$\eta_b(\bar{m}_b(\bar{m}_b))$
$\langle\xi_P^1\rangle_{\rm HP}$	0	0.323 ± 0.025	0
$\langle\xi_P^2\rangle_{\rm HP}$	0.096 ± 0.015	0.253 ± 0.004	0.086 ± 0.010
$\langle\xi_P^3\rangle_{\rm HP}$	0	0.157 ± 0.007	0
$\langle\xi_P^4\rangle_{\rm HP}$	0.023 ± 0.007	0.127 ± 0.002	0.017 ± 0.004
$\langle\xi_P^5\rangle_{\rm HP}$	0	0.094 ± 0.003	0
$\langle\xi_P^6\rangle_{\rm HP}$	0.008 ± 0.003	0.078 ± 0.002	0.005 ± 0.001

TABLE II: The HP twist-3 DA moments $\langle\xi_\sigma^n\rangle_{\rm HP}$ up to $6_{\rm th}$-order. The errors are squared average of those from all input parameters, such as the Borel parameter, the condensates and the bound state parameters. The scale μ is set to be $\bar{m}_c(\bar{m}_c)$ for η_c and $\bar{m}_b(\bar{m}_b)$ for B_c and η_b.

	$\eta_c(\bar{m}_c(\bar{m}_c))$	$B_c(\bar{m}_b(\bar{m}_b))$	$\eta_b(\bar{m}_b(\bar{m}_b))$
$\langle\xi_\sigma^1\rangle_{\rm HP}$	0	0.279 ± 0.023	0
$\langle\xi_\sigma^2\rangle_{\rm HP}$	0.074 ± 0.012	0.182 ± 0.005	0.067 ± 0.007
$\langle\xi_\sigma^3\rangle_{\rm HP}$	0	0.100 ± 0.006	0
$\langle\xi_\sigma^4\rangle_{\rm HP}$	0.015 ± 0.004	0.071 ± 0.003	0.011 ± 0.002
$\langle\xi_\sigma^5\rangle_{\rm HP}$	0	0.047 ± 0.002	0
$\langle\xi_\sigma^6\rangle_{\rm HP}$	0.005 ± 0.002	0.036 ± 0.001	0.003 ± 0.001

We first discuss the properties of the first several moments of the HP twist-3 DA $\phi^P_{3;{\rm HP}}$ and $\phi^\sigma_{3;{\rm HP}}$. Figs.(1, 2) show the stability of those moments versus the Borel parameter M^2, where all input parameters are set to be their central values. Tables I and II display the moments $\langle\xi_P^n\rangle_{\rm HP}$ and $\langle\xi_\sigma^n\rangle_{\rm HP}$ up to $6_{\rm th}$-order, in which the scale μ is set to be $\bar{m}_c(\bar{m}_c)$ for η_c and $\bar{m}_b(\bar{m}_b)$ for B_c and η_b, respectively. In Tables I and II, the errors are squared average of those from all input parameters, such as the Borel parameter, the vacuum condensates and the heavy quark masses. All twist-3 DA moments follow the same trend that a smaller moment is achieved when its order is larger, which explains why people usually only takes into account the first several DA moments to do the discussion. This trend is much more obvious for the cases of η_c and η_b, i.e.

$$\langle\xi_P^2\rangle_{\eta_c(\eta_b)}:\langle\xi_P^4\rangle_{\eta_c(\eta_b)}:\langle\xi_P^6\rangle_{\eta_c(\eta_b)}\simeq 1:0.2:0.08(0.06)$$

and

$$\langle\xi_\sigma^2\rangle_{\eta_c(\eta_b)}:\langle\xi_\sigma^4\rangle_{\eta_c(\eta_b)}:\langle\xi_\sigma^6\rangle_{\eta_c(\eta_b)}\simeq 1:0.2:0.07(0.04).$$

B. Properties of the HP twist-3 DA

TABLE III: The determined model parameters of the HP twist-3 DA $\phi^P_{3;{\rm HP}}$ at the scale $\mu=\bar{m}_b(\bar{m}_b)$.

DA	$\phi^P_{3;\eta_c}$	$\phi^P_{3;B_c}$	$\phi^P_{3;\eta_b}$
$A^P_{\rm HP}({\rm GeV}^{-1})$	2.616	3.101	9.987
$\beta^P_{\rm HP}({\rm GeV})$	3.106	3.626	2.962
$B_1^{{\rm HP},P}$	0	1.378	0
$B_2^{{\rm HP},P}$	0.780	0.744	-1.858
$B_3^{{\rm HP},P}$	0	0.757	0
$B_4^{{\rm HP},P}$	1.920	0.832	0.352
$B_5^{{\rm HP},P}$	0	0.378	0
$B_6^{{\rm HP},P}$	1.021	0.266	0.081

TABLE IV: The determined model parameters of the HP twist-3 DA $\phi^\sigma_{3;{\rm HP}}$ at the scale $\mu=\bar{m}_b(\bar{m}_b)$.

DA	$\phi^\sigma_{3;\eta_c}$	$\phi^\sigma_{3;B_c}$	$\phi^\sigma_{3;\eta_b}$
$A^\sigma_{\rm HP}({\rm GeV}^{-1})$	2.508	3.276	17.235
$\beta^\sigma_{\rm HP}({\rm GeV})$	2.799	3.243	2.773
$B_1^{{\rm HP},\sigma}$	0	0.372	0
$B_2^{{\rm HP},\sigma}$	-0.257	-0.115	-0.359
$B_3^{{\rm HP},\sigma}$	0	-0.085	0
$B_4^{{\rm HP},\sigma}$	0.095	0.009	0.092
$B_5^{{\rm HP},\sigma}$	0	0.002	0
$B_6^{{\rm HP},\sigma}$	-0.010	-0.003	-0.012

By using the moments $\langle\xi_P^n\rangle_{\rm HP}$ and $\langle\xi_\sigma^n\rangle_{\rm HP}$ presented in Tables I and II, we are ready to fix the input parameters for the HP twist-3 DA $\phi^P_{3;{\rm HP}}$ and $\phi^\sigma_{3;{\rm HP}}$. The results of those parameters at the scale $\mu=\bar{m}_b(\bar{m}_b)$ are presented in Tables III and IV, where all input parameters including the moments $\langle\xi_P^n\rangle_{\rm HP}$ and $\langle\xi_\sigma^n\rangle_{\rm HP}$ are set to be their central values. One can get the DA model parameters at any other scales via the evolution equation of the HP DA [15, 25] [2]. For example, at the scale $\mu=\bar{m}_c(\bar{m}_c)$, we have $A^P_{\eta_c}=542.074{\rm GeV}^{-1}$, $B_2^{\eta_c,P}=1.329$, $B_4^{\eta_c,P}=1.219$, $B_6^{\eta_c,P}=0.382$, $\beta^P_{\eta_c}=0.834{\rm GeV}$ for $\phi^P_{3;\eta_c}$; and $A^\sigma_{\eta_c}=736.146{\rm GeV}^{-1}$, $B_2^{\eta_c,\sigma}=0.327$, $B_4^{\eta_c,\sigma}=0.352$, $B_6^{\eta_c,\sigma}=0.108$, $\beta^\sigma_{\eta_c}=0.770{\rm GeV}$ for $\phi^\sigma_{3;\eta_c}$.

We present the twist-3 DAs $\phi^P_{3;{\rm HP}}$ and $\phi^\sigma_{3;{\rm HP}}$ at the scale $\mu=\bar{m}_b(\bar{m}_b)$ in Figs.(3, 4). As required, the η_c and η_b twist-3 DAs are symmetric and the B_c twist-3 DAs are

[2] Another equivalent approach is to evolute the moments $\langle\xi_P^n\rangle_{\rm HP}$ and $\langle\xi_\sigma^n\rangle_{\rm HP}$ listed in Tables I and II to the required scale by using the renormalization group equation for the DA moments [26], and then solve the constraints (3, 4, 5).

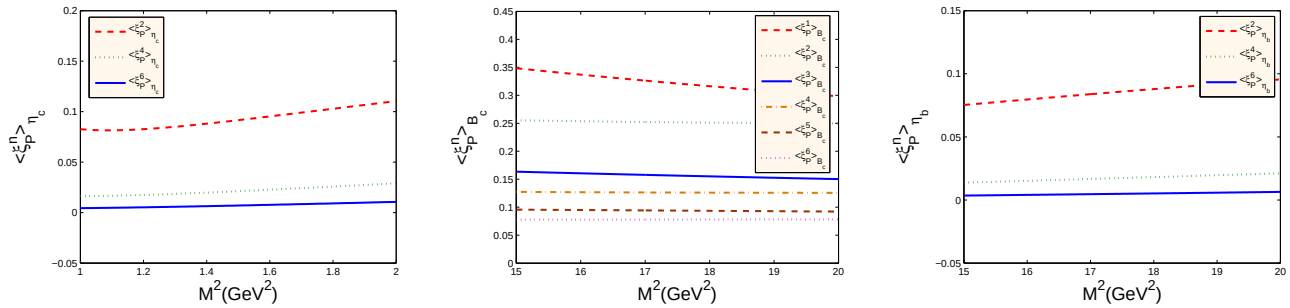

FIG. 1: The moments $\langle \xi_P^n \rangle_{\rm HP}$ $(n \leq 6)$ of the HP twist-3 DA $\phi^P_{3;\rm HP}$ versus the Borel parameter M^2, where all the input parameters are set to be their central values.

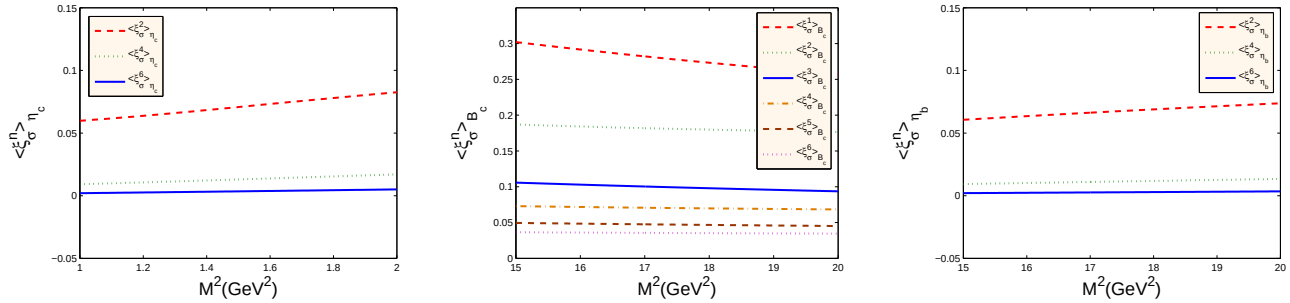

FIG. 2: The moments $\langle \xi_\sigma^n \rangle_{\rm HP}$ $(n \leq 6)$ of the HP twist-3 DA $\phi^\sigma_{3;\rm HP}$ versus the Borel parameter M^2, where all the input parameters are set to be their central values.

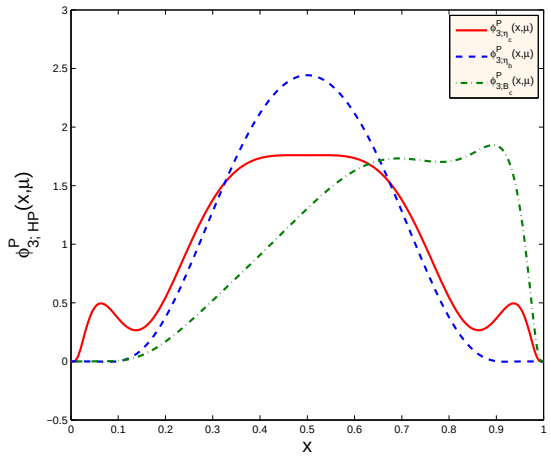

FIG. 3: The curves of the HP twist-3 DA $\phi^P_{3;\rm HP}(x,\mu)$ at the scale $\mu = \bar{m}_b(\bar{m}_b)$.

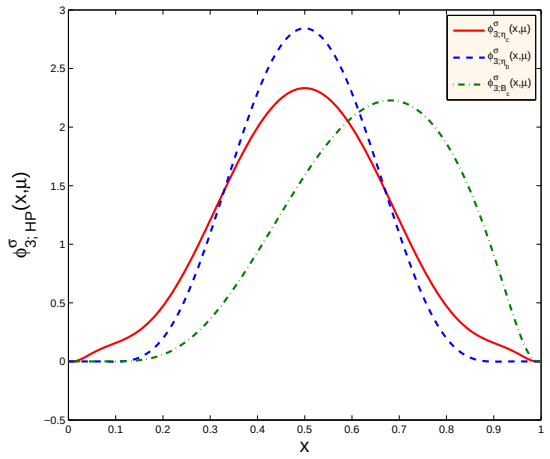

FIG. 4: The curves of the HP twist-3 DA $\phi^\sigma_{3;\rm HP}(x,\mu)$ at the scale $\mu = \bar{m}_b(\bar{m}_b)$.

asymmetric. To show more clearly how those twist-3 DAs change with the scale changes, we present the twist-3 DAs $\phi^P_{3;\rm HP}(x,\mu)$ and $\phi^\sigma_{3;\rm HP}(x,\mu)$ under several typical scales in Figs.(5, 6), where the dashed, the dotted, the dash-dot and the solid lines are for $\mu = \bar{m}_b(\bar{m}_b) = 4.18$GeV, 10GeV, 100GeV and 10000GeV, respectively. In those figures, we also present the results for $\phi^P_{3;\eta_c}$ and $\phi^\sigma_{3;\eta_c}$ at the scale $\mu = \bar{m}_c(\bar{m}_c) = 1.275$GeV. It is found that $\phi^\sigma_{3;\eta_c}$ and $\phi^\sigma_{3;\eta_b}$ are close in shape, both of which tend to the asymptotic form $6x(1-x)$ when $\mu \to \infty$ [25]. $\phi^P_{3;\eta_c}(x,\bar{m}_c(\bar{m}_c))$ and $\phi^P_{3;\eta_b}(x,\bar{m}_b(\bar{m}_b))$ are also close in shape. When $\phi^P_{3;\eta_c}$ and $\phi^P_{3;\eta_b}$ run to high scales, one observes a humped behavior near the end-point region

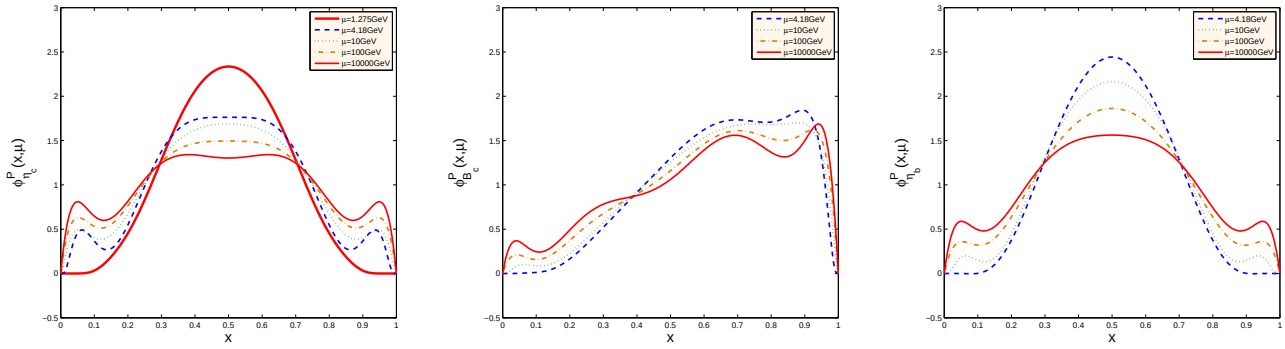

FIG. 5: The running of the HPs' twist-3 DA $\phi^P_{3;\mathrm{HP}}(x,\mu)$. The dashed, the dotted, the dash-dot and the solid lines are for $\mu = 4.18$GeV, 10GeV, 100GeV and 10000GeV, respectively. Moreover, in the first figure the thick solid line is for $\mu = 1.275$GeV.

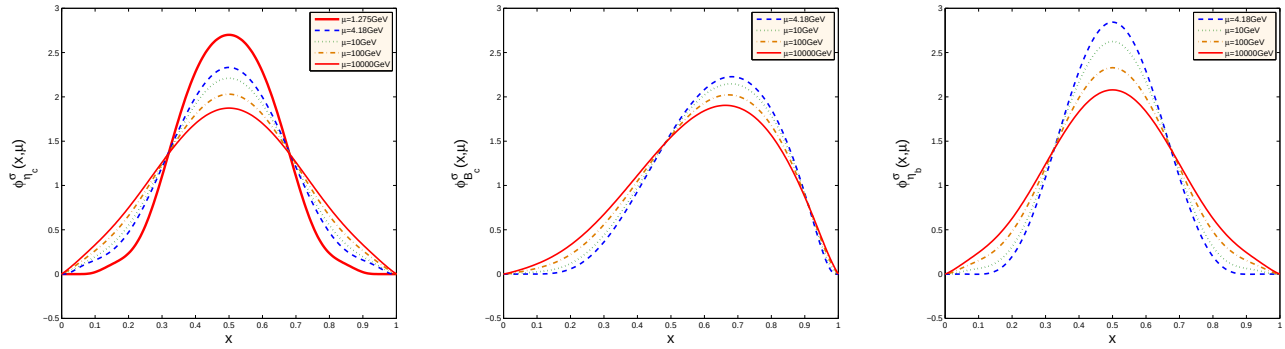

FIG. 6: The running of the HPs' twist-3 DA $\phi^\sigma_{3;\mathrm{HP}}(x,\mu)$. The dashed, the dotted, the dash-dot and the solid lines are for $\mu = 4.18$GeV, 10GeV, 100GeV and 10000GeV, respectively. Moreover, in the first figure the thick solid line is for $\mu = 1.275$GeV.

$x \to 0$ or 1 [3]. Such humped behavior can be explained as a combination effect of the asymptotic behavior $\phi^P_{3;\eta_{c(b)}}(x,\mu\to\infty) = 1$ and the end-point suppression as indicated by Eq.(1).

IV. THE APPLICATION OF THE HP TWIST-3 DA TO THE TFF $f_+^{B_c\to\eta_c}(q^2)$

In the literature, in order to suppress the contributions from the higher-twist DA, which are uncertain and less-known, people have suggested to use a chiral correlator other than the conventional correlator to do the light-cone sum rules (LCSR) calculation [27]. In addition to the $B\to\pi$ transition [28–30], this method has also been applied to other transitions such as the $B(D)\to\pi$ transition [31], the $B\to K$ transition [32, 33], the $B(B_s, B_c)\to P(V)$ transition [34–36], the $B\to D$ transition [37], the $B\to S$ transition [38] and etc. In Ref.[15], we have adopted the chiral correlator for the TFF $f_+^{B_c\to\eta_c}(q^2)$, which does only contain the η_c leading-twist DA in the LCSR. In this section, as an application of the present suggested HP twist-3 DA model, we shall calculate the TFF $f_+^{B_c\to\eta_c}(q^2)$ by using the conventional correlator to do our LCSR discussion, in which both the twist-2 and twist-3 terms have been kept.

A. Properties of the LCSR prediction of $f_+^{B_c\to\eta_c}(q^2)$ with the conventional correlator

The $B_c\to\eta_c$ TFF $f_+^{B_c\to\eta_c}(q^2)$ is defined by the following matrix element

$$\langle\eta_c(p)\,|\bar{c}\gamma_\mu b|\,B_c(p+q)\rangle = 2f_+^{B_c\to\eta_c}(q^2)p_\mu + \left[f_+^{B_c\to\eta_c}(q^2) + f_-^{B_c\to\eta_c}(q^2)\right]q_\mu. \quad (18)$$

By using the conventional correlator

$$\Pi_\mu(p,q) = i\int d^4x e^{iq\cdot x}\left\langle\eta_c(p)\left|\bar{c}(x)\gamma_\mu b(x),(m_b+m_c)\bar{b}(0)i\gamma_5 c(0)\right|0\right\rangle$$

[3] Because the c-quark is lighter than the b-quark, $\phi^P_{3;\eta_c}$ shows the humped behavior more quickly with the increment of scale than $\phi^P_{3;\eta_b}$ and is more transparent at the same scale.

$$= F\left[(p+q)^2\right] p_\mu + q_\mu \text{terms},$$

and following the standard procedure of the LCSR approach [39–41], one can obtain the LCSR of $f_+^{B_c\to\eta_c}(q^2)$, which can be formulated as a function of η_c twist-2 and twist-3 DAs, i.e.

$$\begin{aligned} f_+^{B_c\to\eta_c}(q^2) &= \frac{m_b(m_b+m_c)f_{\eta_c}}{2m_{B_c}^2 f_{B_c}} e^{m_{B_c}^2/M^2} \\ &\times \int_\Delta^1 du e^{-\frac{m_b^2-\bar{u}q^2+u\bar{u}m_{\eta_c}^2}{uM^2}} \left\{ \frac{\phi_{2;\eta_c}(u)}{u} + \frac{\mu_{\eta_c}}{m_b} \right. \\ &\times \left[\phi_{3;\eta_c}^P(u) + \frac{1}{6}\left(1-\frac{4m_c^2}{m_{\eta_c}^2}\right) \right. \\ &\times \left(\frac{2\phi_{3;\eta_c}^\sigma(u)}{u} + \frac{1}{m_b^2-q^2+u^2m_{\eta_c}^2} \right. \\ &\times \left[\frac{4um_b^2m_{\eta_c}^2}{m_b^2-q^2+u^2m_{\eta_c}^2}\phi_{3;\eta_c}^\sigma(u) \right. \\ &- \left. \left. \left. (m_b^2+q^2-u^2m_{\eta_c}^2)\frac{d\phi_{3;\eta_c}^\sigma(u)}{du} \right] \right) \right] \left. \right\}, \end{aligned} \tag{20}$$

where $\phi_{2;\eta_c}(u)$ is the leading-twist DA of η_c, $\bar{u}=1-u$, and

$$\begin{aligned} \Delta &= \left[\sqrt{(s_0-q^2-m_{\eta_c}^2)^2+4m_{\eta_c}^2(m_b^2-q^2)} \right. \\ &- \left. (s_0-q^2-m_{\eta_c}^2) \right] / \left(2m_{\eta_c}^2\right). \end{aligned} \tag{21}$$

TABLE V: A comparison of the $B_c\to\eta_c$ TFF $f_+^{B_c\to\eta_c}(0)$ under various approaches, i.e. the LCSR, the QCD sum rules (SR), the quark model (QM), the Bauer-Stech-Wirbel (BSW) framework, the perturbative QCD (pQCD) approach and the non-relativistic QCD (NRQCD) appraoch.

Approach	$f_+^{B_c\to\eta_c}(0)$	Ref.
LCSR	0.674 ± 0.066	This work
	$0.612^{+0.053}_{-0.052}$	[15]
QCD SR	0.66	[42]
QM	0.61	[43]
	$0.49^{+0.01}$	[44]
	$0.61^{+0.03+0.01}_{-0.04-0.01}$	[47]
	0.47	[48]
BSW	$0.58^{+0.02}_{-0.01}$	[45]
LO pQCD	$0.48\pm0.06\pm0.01$	[46]
NLO NRQCD	1.65	[49]
	1.28	[50] [a]

[a] This value is obtained by using the formulas of Ref.[50] but with the same parameter values of Ref.[49].

To do the numerical calculation, the η_c twist-2 DA constructed in Ref.[15] and the η_c twist-3 DA as shown by Eq.(1) are adopted. As for its continuum threshold parameter and the Borel window, we take them to be $s_0=42\text{GeV}^2$ and $M^2=(20-35)\text{GeV}^2$. At the maximum recoil region, we obtain

$$f_+^{B_c\to\eta_c}(0)=0.674\pm0.066, \tag{22}$$

where all the theoretical uncertainties such as those from the Borel parameter and the bound state parameters have been added up in quadrature. A comparison of $f_+^{B_c\to\eta_c}(0)$ under various approaches [15, 42–50] is put in Table V, where 'LO' is the leading-order prediction and 'NLO' is the next-to-leading order prediction. The predictions from the LCSR, the quark model and the Bauer-Stech-Wirbel framework are at the LO level, most of them are consistent with each other within reasonable theoretical errors. The NLO NRQCD predictions are much bigger [49, 50], indicating the importance of the NLO-terms. Moreover, Ref.[49] shows the necessity of a proper renormalization scale-setting, i.e. it is important to achieve a reliable lower-order prediction.

By using the branching ratio formulas listed in Ref.[15] but with the present LCSR for $f_+^{B_c\to\eta_c}(q^2)$, we finally predict the branching ratio of $B_c\to\eta_c l\nu$ as

$$Br(B_c\to\eta_c l\nu)=(9.31^{+2.27}_{-2.01})\times10^{-3}, \tag{23}$$

where the error of the branching ratio originates mainly from the TFF $f_+^{B_c\to\eta_c}(q^2)$, the CKM matrix element $|V_{cb}|$ and the B_c meson lifetime τ_{B_c}. The advantage of LCSR prediction in comparison to the pQCD ones lies in that the LCSRs is valid in a broader region $0<q^2<m_b^2-2m_b\Lambda_{\rm QCD}\simeq15\text{GeV}^2$, which is close to the allowable phase-space of $B_c\to\eta_c l\nu$, thus one may directly apply the LCSR prediction of $f_+^{B_c\to\eta_c}(q^2)$ to calculate the branching ratio $Br(B_c\to\eta_c l\nu)$; while, the pQCD prediction is only reliable in low q^2-region around the maximum recoil point, thus certain extrapolation must be applied, different choice of which shall introduce large extra error into the prediction.

B. A comparison of the LCSRs under various correlators and the HP twist-3 DA

Table V shows at the large recoil region, the two LCSR predictions and also the QCD sum rules prediction agree with each other within reasonable theoretical errors. A comparison of the LCSR predictions of $f_+^{B_c\to\eta_c}(q^2)$ under the conventional and the chiral correlators are shown in Fig.(7), where the shaded hands are their uncertainties. Fig.(7) shows the consistency of those two LCSR predictions is satisfied for all q^2-region. In Ref.[15] a chiral correlator is adopted such that to suppress (or even eliminate) the unknown higher-twist contributions. In the present paper, we have shown that if one can construct a proper model for the twist-3 DA, one can also get a more accurate LCSR prediction.

By using the LCSR with the conventional correlator, it is interesting to show what are the contributions for the TFF $f_+^{B_c\to\eta_c}(q^2)$ from different twist DA. We present the LCSR of $f_+^{B_c\to\eta_c}(q^2)$ versus q^2 in Fig.(8), where the contributions from $\phi_{2;\eta_c}$, $\phi_{3;\eta_c}^P$ and $\phi_{3;\eta_c}^\sigma$ are shown explicitly. The shaded hand shows its uncertainties, where all the errors have been added up in quadrature. At $q^2=0$, if set-

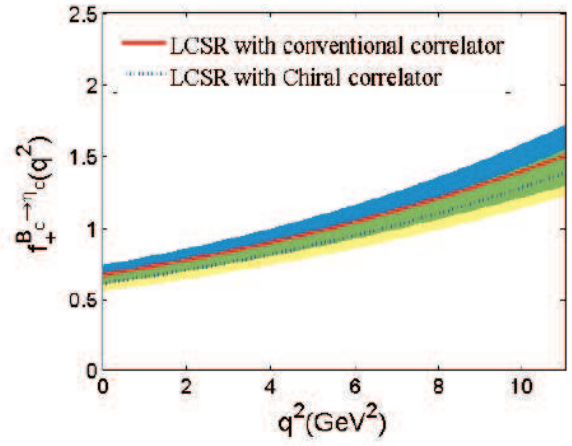

FIG. 7: A comparison of the LCSR predictions of $f_+^{B_c\to\eta_c}(q^2)$ under two different correlators, where the shaded hands are their uncertainties. The thicker shaded band stands for the LCSR with the chiral correlator and the lighter one stands for the LCSR with the conventional correlator. The dashed and solid lines are for their central values, respectively.

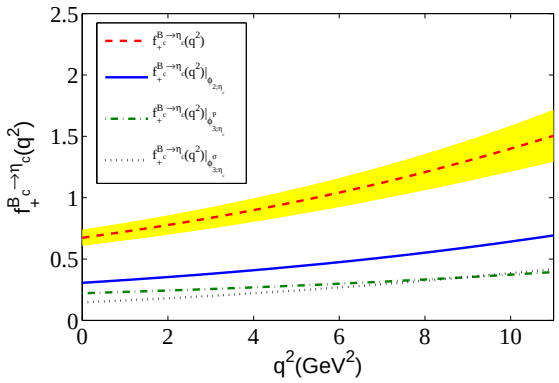

FIG. 8: The LCSR with the conventional correlator for the TFF $f_+^{B_c\to\eta_c}(q^2)$ versus q^2, where the shaded hand is its uncertainty. The solid, the dash-dot, the dotted and the dashed lines are for $\phi_{2;\eta_c}$, $\phi^P_{3;\eta_c}$, $\phi^\sigma_{3;\eta_c}$ and their sums, respectively.

ting all the parameters to be their central values, we have $f_+^{B_c\to\eta_c}(0)|_{\phi_{2;\eta_c}} = 0.306$, $f_+^{B_c\to\eta_c}(0)|_{\phi^P_{3;\eta_c}} = 0.221$ and $f_+^{B_c\to\eta_c}(0)|_{\phi^\sigma_{3;\eta_c}} = 0.147$, whose proportions in $f_+^{B_c\to\eta_c}(0)$ are 45%, 33% and 22%, respectively. This shows the twist-3 contributions are large and important. For any other q^2-values, even though the twist-3 contribution become smaller, the conditions are similar. Moreover, when the value of q^2 increases, the twist-2 contribution increases faster, for a large enough q^2-value, e.g. $q^2 > 10$ GeV^2, we roughly have

$$q^2\frac{f_+^{B_c\to\eta_c}(q^2)|_{\phi^P_{3;\eta_c}}}{f_+^{B_c\to\eta_c}(q^2)|_{\phi_{2;\eta_c}}} \rightsquigarrow \text{ a flat line}, \tag{24}$$

$$q^2\frac{f_+^{B_c\to\eta_c}(q^2)|_{\phi^P_{3;\eta_c}}}{f_+^{B_c\to\eta_c}(q^2)|_{\phi_{2;\eta_c}}} \rightsquigarrow \text{ a flat line}, \tag{25}$$

indicating that the twist-3 contributions satisfy the usual q^2-suppression to the leading twist-2 contribution in large q^2-region. This in some sense shows the importance of the twist-3 DA with better end-point behavior. In fact, if taking $\phi^P_{3;\eta_c}$ to be its asymptotic form that has no end-point suppression, $\phi^P_{3;\eta_c}(x) \equiv 1$, one cannot obtain such a q^2-suppression and the $\phi^P_{3;\eta_c}$ contribution shall be even dominant over the twist-2 one. This condition is similar to the case of $B \to \pi$ decays [16] and the pion form factor [51] , only if one has used a $\phi^P_{3;\pi}$ with better end-point behavior can one achieve the required power-suppressed twist-3 contribution.

V. SUMMARY

In this paper, based on the BHL-prescription, we have constructed a new model for the twist-3 DA $\phi^P_{3;\rm HP}$ and $\phi^\sigma_{3;\rm HP}$, which are for η_c, B_c and η_b, respectively. To fit the parameters, we have calculated their moments $\langle\xi^n_P\rangle_{\rm HP}$ and $\langle\xi^n_\sigma\rangle_{\rm HP}$ by using the QCD SVZ sum rules under the framework of BFT. Tables I and II display the values of those moments up to $6_{\rm th}$-order, which become smaller when they are at higher orders.

As an application of the constructed HP twist-3 DA, we have calculated the $B_c \to \eta_c$ TFF $f_+^{B_c\to\eta_c}$ by applying the LCSR with the conventional correlator. At the maximum recoil point, we obtain $f_+^{B_c\to\eta_c}(0) = 0.674 \pm 0.066$, which agrees with the predictions of other approaches also at the leading-order level. We have found that the net contributions from the η_c twist-3 DA are large, which is up to 55% for $f_+^{B_c\to\eta_c}(0)$. Such an importance of twist-3 DA can also be extended to other q^2-values as shown by Fig.(8). Furthermore, we have calculated the branching ratio of $B_c \to \eta_c l\nu$, $Br(B_c \to \eta_c l\nu) = (9.31^{+2.27}_{-2.01}) \times 10^{-3}$, which is consistent with the previous LCSR prediction [15]. Being with a good end-point behavior due to the BHL-prescription, our present twist-3 contributions satisfy the usual q^2-suppression to the leading twist-2 contribution in large q^2-region.

The HP twist-3 DA are important inputs for analyzing the high-energy processes involving the HP, thus we think our present model shall have wide applications.

Acknowledgments: This work was supported in part by the Natural Science Foundation of China under Grants No.11547015, No.11235005, No.11575110, No.11275280, and No.11547305, and by Fundamental Research Funds for the Central Universities under Grant No.CDJZR305513.

Appendix: The expressions of $\mathrm{Im}I^{\mathrm{PS,PT}}_{\mathrm{HP,pert}}(s)$, $I^{\mathrm{PS,PT}}_{\mathrm{HP},\langle G^2\rangle}(M^2)$ and $I^{\mathrm{PS,PT}}_{\mathrm{HP},\langle G^3\rangle}(M^2)$

In this appendix, we list the necessary expressions for deriving the sum rules of the moments $\langle\xi^n_P\rangle_{\mathrm{HP}}$ and $\langle\xi^n_\sigma\rangle_{\mathrm{HP}}$, which are

$$
\begin{aligned}
\mathrm{Im}I^{\mathrm{PS}}_{\mathrm{HP,pert}}(s) &= \frac{3\bar{s}}{16\pi(n+1)}\left[\left(\frac{-m_1^2+m_2^2+\bar{s}v}{s}\right)^{n+1}-\left(\frac{-m_1^2+m_2^2-\bar{s}v}{s}\right)^{n+1}\right], \qquad (26)\\
I^{\mathrm{PS}}_{\mathrm{HP},\langle G^2\rangle}(M^2) &= \left\langle\alpha_s G^2\right\rangle\int_0^1 dx(2x-1)^n\exp\left[-\frac{m_1^2x+m_2^2(1-x)}{M^2x(1-x)}\right]\left\{\frac{n+1}{M^2}\left(\frac{1}{12\pi}n(n-1)(2x-1)^{-2}x(1-x)\right.\right.\\
&+ \left.\frac{1}{8\pi}\right)+\frac{1}{M^4x^2(1-x)^2}\left(-\frac{1}{24\pi}\left[nm_1^2x^3+nm_2^2(1-x)^3+2m_1m_2(nx(1-x)-x^2-(1-x)^2)\right]\right.\\
&+ \frac{1}{12\pi}n(n-1)(2x-1)^{-2}x^2(1-x)^2(m_1+m_2)[m_1x+m_2(1-x)]+\frac{1}{8\pi}x(1-x)\left[m_1^2x+m_2^2(1-x)\right.\\
&+ \left.\left.2m_1m_2\right])+\frac{1}{2M^6x^3(1-x)^3}\left(-\frac{1}{12\pi}\left[m_1^4x^4+m_2^4(1-x)^4+m_1m_2x(1-x)(m_1^2x+m_2^2(1-x))\right.\right.\right.\\
&+ \left.\left.\left.m_1^2m_2^2x(1-x)(x^2+(1-x)^2)\right]\right)\right\},\\
I^{\mathrm{PS}}_{\mathrm{HP},\langle G^3\rangle}(M^2) &= \left\langle g_s^3fG^3\right\rangle\int_0^1(2x-1)^n\exp\left[-\frac{m_1^2x+m_2^2(1-x)}{M^2x(1-x)}\right]\left\{\frac{1}{M^4x^2(1-x)^2}\left(\frac{-9n}{1024\pi^2}\left[\frac{1}{32}n(n-1)(2x-1)^{-2}\right.\right.\right.\\
&+ \left.\left.6-\frac{1}{32}n(n-1)+x(1-x)\left(-\frac{1}{8}n(n+63)-22+\frac{3}{2}(n+1)(n+6)x(1-x)\right)\right]+\frac{7}{2304\pi^2}n(n-1)\right.\\
&\times \left.(2x-1)^{-2}x(1-x)\left[2(n+2)x(1-x)-3\right]+\frac{1}{144\pi^2}n(n-1)(2x-1)^{-2}x(1-x)[x^2+(1-x)^2]\right.\\
&- \left.\frac{1}{576\pi^2}(n+1)n^2(n-1)(2x-1)^{-2}x^3(1-x)^3-\frac{7}{1536\pi^2}nx(1-x)[3-2(n+1)x(1-x)]-\frac{1}{96\pi^2}n\right.\\
&\times \left.(n-1)(2x-1)^{-2}x^2(1-x)^2-\frac{1}{144\pi^2}x(1-x)\left[-\frac{1}{4}n(n-1)(2x-1)^{-2}+\frac{1}{4}n(n-1)-3-6n\,(n\right.\right.\\
&+ \left.\left.1)\,x(1-x)\right])+\frac{1}{2M^6x^3(1-x)^3}\left(\frac{-1}{15360\pi^2}\left[6m_1^2x\left(\left(\frac{143}{32}n(n-1)-\frac{49}{8}n(n-1)x\right)(2x-1)^{-2}\right.\right.\right.\\
&+ \left.\frac{49}{8}(n-1)(n+24)x-\frac{143}{32}n(n-1)+270+x(1-x)\left(-\frac{147}{2}(n-1)(n+2)x-\frac{n}{8}(143n+5353)\right.\right.\\
&- \left.\left.663+\frac{n}{2}(413n+1477)x(1-x)\right)\right)+6m_2^2(1-x)\left(\left(\frac{143}{32}n(n-1)-\frac{49}{8}n(n-1)(1-x)\right)(2x-1)^{-2}\right.\\
&+ \left.\frac{49}{8}(n-1)(n+24)(1-x)-\frac{143}{32}n(n-1)+270+x(1-x)\left(-\frac{147}{2}(n-1)(n+2)(1-x)-\frac{n}{8}\,(143n\right.\right.\\
&+ \left.\left.5353)-663+\frac{n}{2}(413n+1477)x(1-x)\right)\right)+268m_1m_2\left(\frac{1}{32}n(n-1)(2x-1)^{-2}-\frac{1}{32}n(n-1)+3\right.\\
&+ \left.\left.x(1-x)\left(-\frac{1}{8}n(n+47)-6+\frac{3}{2}(n-1)(n+4)x(1-x)\right)\right)\right]-\frac{1}{2304\pi^2}n(n-1)(2x-1)^{-2}x(1-x)\\
&\times \left[2m_1^2x^2(36x-7)+2m_2^2(1-x)^2(36(1-x)-7)\right]+\frac{1}{72\pi^2}n(n-1)(2x-1)^{-2}x(1-x)\left[m_1^2x^3+m_2^2\right.\\
&\times \left.(1-x)^3-m_1m_2x(1-x)\right]-\frac{1}{288\pi^2}n(n-1)(2x-1)^{-2}x^3(1-x)^3\left[2nm_1^2x+2nm_2^2(1-x)+(n\right.\\
&- \left.1)\,m_1m_2\right]-\frac{1}{768\pi^2}x(1-x)\left[m_1^2x\left(-28nx(1-x)+37(n-1)x+21\right)+m_2^2(1-x)\left(-28nx(1-x)\right.\right.\\
&+ \left.\left.37(n-1)(1-x)+21\right)-32m_1m_2\left(1-(n-1)x(1-x)\right)\right]-\frac{1}{48\pi^2}x(1-x)\left[m_1^2x\left(-\frac{n}{2}(2x-1)^{-1}\right.\right.
\end{aligned}
$$

$$
\begin{aligned}
&- \ 8nx(1-x)+(n-1)x-\frac{n+2}{2}\Big)+m_2^2(1-x)\left(\frac{n}{2}(2x-1)^{-1}-8nx(1-x)+(n-1)(1-x)\right.\\
&- \ \left.\frac{n+2}{2}\Big)-8(n-1)m_1m_2x(1-x)\Big]\right)+\frac{1}{6M^8x^4(1-x)^4}\left(\frac{-1}{5120\pi^2}\left[m_1^4x^3\left(-\frac{147n}{4}(2x-1)^{-1}\right.\right.\right.\\
&+ \ \left.\left.\left.\left(\frac{433n}{2}+1676\right)x-\frac{147n}{4}-1080+x(1-x)\left(-(1263n+1572)x+385n+1564\right)\right)+m_2^4(1-x)^3\right.\right.\\
&\times \ \left.\left.\left(\frac{147n}{4}(2x-1)^{-1}+\left(\frac{433n}{2}+1676\right)(1-x)-\frac{147n}{4}-1080+x(1-x)\left(-(1263n+1572)(1-x)\right.\right.\right.\right.\\
&+ \ \left.\left.\left.\left.385n+1564\right)\right)+4m_1^3m_2x^2\left(-\frac{87n}{8}(2x-1)^{-1}+\left(\frac{87n}{4}+375\right)x-\frac{87n}{8}-201+x(1-x)\right.\right.\right.\\
&\times \ \left.\left.\left.\left(-(221n+161)x+\frac{181n}{2}+161\right)\right)+4m_1m_2^3(1-x)^2\left(\frac{87n}{8}(2x-1)^{-1}+\left(\frac{87n}{4}+375\right)(1-x)\right.\right.\right.\\
&- \ \left.\left.\left.\frac{87n}{8}-201+x(1-x)\left(-(221n+161)(1-x)+\frac{181n}{2}+161\right)\right)+6m_1^2m_2^2x(1-x)\left((421n+524)\right.\right.\right.\\
&\times \ \left.\left.\left.x^2(1-x)^2-(147n+703)x(1-x)+147\right)\right]-\frac{1}{144\pi^2}n(n-1)(2x-1)^{-2}x^3(1-x)^3\left[(m_1+m_2)\right.\right.\\
&\times \ \left.\left.(m_1x+m_2(1-x))(m_1^2x+m_2^2(1-x))\right]-\frac{1}{256\pi^2}x(1-x)\left[m_1^4x^3(14x+23)+m_2^4(1-x)^3\left(14(1-x)\right.\right.\right.\\
&+ \ \left.\left.\left.23\right)+2m_1^3m_2x^2(-16x+45)+2m_1m_2^3(1-x)^2(-16(1-x)+45)+m_1^2m_2^2x(1-x)\left(-28x(1-x)\right.\right.\right.\\
&+ \ \left.\left.\left.37\right)\right]-\frac{1}{16\pi^2}x(1-x)\left[m_1^4x^3(4x-3)+m_2^4(1-x)^3(4(1-x)-3)-8m_1^3m_2x^2(1-x)-8m_1m_2^3x\right.\right.\\
&\times \ \left.\left.(1-x)^2-m_1^2m_2^2x(1-x)(1+8x(1-x))\right]\right)+\frac{1}{1280\pi^2\times 24M^{10}x^5(1-x)^5}\left[m_1^6x^5\left(429x(1-x)\right.\right.\\
&- \ \left.\left.8x-135\right)+m_2^6(1-x)^5\left(429x(1-x)-8(1-x)-135\right)+2m_1^5m_2x^4\left(241x(1-x)-32x-67\right)\right.\\
&+ \ \left.2m_1m_2^5(1-x)^4\left(241x(1-x)-32(1-x)-67\right)+m_1^4m_2^2x^3(1-x)\left(1287x^2(1-x)-850x(1-x)\right)\right.\\
&- \ \left.437x+294\right)+m_1^2m_2^4x(1-x)^3\left(1287x(1-x)^2-850x(1-x)-437(1-x)+294\right)+4m_1^3m_2^3x^2\\
&\times \ \left.(1-x)^2(-241x(1-x)+87)\right]\Big\}\,.
\end{aligned}
$$

$$
\begin{aligned}
\mathrm{Im}I^{\mathrm{PT}}_{\mathrm{HP,pert}}(s) \ &= \ \frac{-3}{16\pi(n+1)(n+2)(n+3)}(n+1)\left\{\left(\frac{-m_1^2+m_2^2+\bar{s}v}{s}\right)^{n+2}\left[-m_1^2+m_2^2-(n+2)\bar{s}v\right]\right.\\
&- \ \left.\left(\frac{-m_1^2+m_2^2-\bar{s}v}{s}\right)^{n+2}\left[-m_1^2+m_2^2+(n+2)\bar{s}v\right]\right\},\\
I^{\mathrm{PT}}_{\mathrm{HP},\langle \mathrm{G}^2\rangle}(M^2) \ &= \ -\left\langle\alpha_sG^2\right\rangle(n+1)\int_0^1 dx(2x-1)^n\exp\left[-\frac{m_1^2x+m_2^2(1-x)}{M^2x(1-x)}\right]\left\{\frac{1}{M^2}\left(-\frac{1}{12\pi}n(n-1)(2x-1)^{-2}x\right.\right.\\
&\times \ \left.\left.(1-x)-\frac{1}{24\pi}\right)+\frac{1}{M^4x^2(1-x)^2}\left(\frac{1}{24\pi}\left[m_1^2x^3+m_2^2(1-x)^3\right]-\frac{1}{12\pi}m_1m_2x(1-x)\right)\right\},\\
I^{\mathrm{PT}}_{\mathrm{HP},\langle \mathrm{G}^3\rangle}(M^2) \ &= \ -\left\langle g_s^3fG^3\right\rangle(n+1)\int_0^1 dx(2x-1)^n\exp\left[-\frac{m_1^2x+m_2^2(1-x)}{M^2x(1-x)}\right]\left\{\frac{1}{M^4x^2(1-x)^2}\left(\frac{9}{1024\pi^2}\left[\frac{1}{32}n(n-1)\right.\right.\right.\\
&\times \ \left.\left.\left.(2x-1)^{-2}-\frac{1}{32}n(n-1)+6+x(1-x)\left(-\frac{1}{8}n(n+63)-22+\frac{3}{2}(n+1)(n+6)x(1-x)\right)\right]\right.\\
&+ \ \left.\frac{7}{2304\pi^2}(n+1)x(1-x)[3-2(n+4)x(1-x)]+\frac{1}{144\pi^2}x(1-x)\left[4(n+1)x(1-x)-n-2\right]\right.\\
&+ \ \left.\frac{1}{576\pi^2}(n+1)n(n-1)(2x-1)^{-2}x^3(1-x)^3+\frac{7}{4608\pi^2}x(1-x)[2(n+1)x(1-x)-3]+\frac{1}{144\pi^2}\right.\\
&\times \ \left.(n+1)x^2(1-x)^2\right)+\frac{1}{2M^6x^3(1-x)^3}\left(\frac{1}{2560\pi^2}\left[m_1^2x^2\left(-\frac{49n}{8}(2x-1)^{-1}-\frac{49n}{8}-180+\left(\frac{49n}{4}\right.\right.\right.\right.\\
&+ \ \left.\left.\left.\left.327\right)x+x(1-x)\left(-(139n+405)x+\frac{131n}{2}+258\right)\right)+m_2^2(1-x)^2\left(\frac{49n}{8}(2x-1)^{-1}-\frac{49n}{8}\right.\right.\right.
\end{aligned}
$$

$$
\begin{aligned}
&- \quad 180+\left(\frac{49n}{4}+327\right)(1-x)+x(1-x)\left(-(139n+405)(1-x)+\frac{131n}{2}+258\right)\Big)\Big]+\frac{1}{1152\pi^2}\\
&\times\ x(1-x)\left[m_1^2x\left(-(50n+56)x(1-x)+29nx+21\right)+m_2^2(1-x)\left(-(50n+56)x(1-x)+29n\right.\right.\\
&\times\quad \left.\left.(1-x)+21\right)+2m_1m_2\left((15n+16)x(1-x)-8\right)\right]+\frac{1}{72\pi^2}x(1-x)\left[m_1^2x\left(\frac{n}{4}(2x-1)^{-1}+(2n+4)\right.\right.\\
&\times\ \left.\left.x(1-x)-\frac{3n}{2}x+\frac{n}{4}-2\right)+m_2^2(1-x)\left(-\frac{n}{4}(2x-1)^{-1}+(2n+4)x(1-x)-\frac{3n}{2}(1-x)+\frac{n}{4}-2\right)\right.\\
&-\quad \left.9nm_1m_2x(1-x)\right]+\frac{11}{192\pi^2}nm_1m_2x^2(1-x)^2+\frac{1}{288\pi^2}n(n-1)(2x-1)^{-2}x^3(1-x)^3\left[m_1^2x+m_2^2\right.\\
&\times\ \left.(1-x)\right]-\frac{7}{2304\pi^2}x(1-x)\left[m_1^2x^2(2x+1)+m_2^2(1-x)^2(2(1-x)+1)\right]-\frac{1}{24\pi^2}m_1m_2x^2(1-x)^2\\
&+\quad \left.\frac{1}{72\pi^2}x^2(1-x)^2\left[m_1^2x+m_2^2(1-x)+3m_1m_2\right]\right)+\frac{1}{6M^8x^4(1-x)^4}\left(\frac{1}{5120\pi^2}\left[m_1^4x^4\left(-429x(1-x)\right.\right.\right.\\
&+\quad \left.\left.\left.8x+135\right)+m_2^4(1-x)^4\left(-429x(1-x)+8(1-x)+135\right)+6m_1^2m_2^2x^2(1-x)^2\left(143x(1-x)-49\right)\right]\right.\\
&+\quad \left.\frac{1}{384\pi^2}x(1-x)\left[m_1^4x^3(36x-7)+m_2^4(1-x)^3(36(1-x)-7)+m_1^3m_2x^2(14x+15)+m_1m_2^3(1-x)^2\right.\right.\\
&\times\ \left.\left.(14(1-x)+15)+m_1^2m_2^2x(1-x)(29-72x(1-x))\right]-\frac{1}{12\pi^2}x(1-x)(m_1^2x+m_2^2(1-x))\left[m_1^2x^3\right.\right.\\
&+\quad \left.\left.\left.m_2^2(1-x)^3+3m_1m_2x(1-x)\right]+\frac{11}{64\pi^2}x^2(1-x)^2m_1m_2[m_1^2x+m_2^2(1-x)]\right)\right\}.
\end{aligned}
$$

Where $\bar{s}=s-(m_1-m_2)^2$ and $v^2=1-4m_1m_2/\bar{s}$.

[1] G. Bell and Th. Feldmann, "Modelling light-cone distribution amplitudes from non-relativistic bound states", JHEP **0804**, 061 (2008).

[2] H. Kawamura, J. Kodaira, C. F. Qiao and K. Tanaka, "B meson light cone distribution amplitudes in the heavy quark limit," Phys. Lett. B **523**, 111 (2001).

[3] T. Huang, C. F. Qiao and X. G. Wu, "B-meson wavefunction with 3-particle Fock states' contributions," Phys. Rev. D **73**, 074004 (2006).

[4] A. E. Bondar and V. L. Chernyak, "Is the BELLE result for the cross section $\sigma(e^+e^-\to J/\psi+\eta_c)$ a real difficulty for QCD?", Phys. Lett. B **612**, 215 (2005).

[5] G. T. Bodwin, D. Kang and J. Lee, "Reconciling the light-cone and NRQCD approaches to calculating $e^+e^-\to J/\psi+\eta_c$", Phys. Rev. D **74**, 114028 (2006).

[6] J. P. Ma and Z. G. Si, "NRQCD Factorization for Twist-2 Light-Cone Wave-Functions of Charmonia", Phys. Lett. B **647**, 419 (2007).

[7] V. V. Braguta, A. K. Likhoded and A. V. Luchinsky, "The Study of leading twist light cone wave function of η_c meson", Phys. Lett. B **646**, 80 (2007).

[8] T. Huang and F. Zuo, "Semileptonic B_c decays and charmonium distribution amplitude", Eur. Phys. J. C **51**, 833 (2007).

[9] X. G. Wu and T. Huang, "Heavy and light meson wavefunctions", Chin. Sci. Bull. **59**, 3801 (2014).

[10] Y. J. Sun, X. G. Wu, F. Zuo and T. Huang, "The Cross section of the process e+ + e- → J/psi+ eta(c) within the QCD light-cone sum rules," Eur. Phys. J. C **67**, 117 (2010).

[11] J. Govaerts, F. de Viron, D. Gusbin and J. Weyers, "Exotic Mesons From QCD Sum Rules", Phys. Lett. B **128**, 262 (1983).

[12] J. Govaerts, F. de Viron, D. Gusbin and J. Weyers, "QCD Sum Rules and Hybrid Mesons", Nucl. Phys. B **248**, 1 (1984);

[13] T. Huang and Z. Huang, "Quantum Chromodynamics in Background Fields", Phys. Rev. D **39**, 1213 (1989).

[14] M. A. Shifman, A. I. Vainshtein and V. I. Zakharov, "QCD and Resonance Physics. Theoretical Foundations", Nucl. Phys. B **147**, 385 (1979).

[15] T. Zhong, X. G. Wu and T. Huang, "Heavy Pseudoscalar Leading-Twist Distribution Amplitudes within QCD Theory in Background Fields", Eur. Phys. J. C **75**, 45 (2015).

[16] T. Huang and X. G. Wu, "Consistent calculation of the B to pi transition form-factor in the whole physical region," Phys. Rev. D **71**, 034018 (2005).

[17] T. Kurimoto, "Uncertainty in the leading order PQCD calculations of B meson decays," Phys. Rev. D **74**, 014027 (2006).

[18] H. N. Li, S. Mishima and A. I. Sanda, "Resolution to the B → pi K puzzle," Phys. Rev. D **72**, 114005 (2005).

[19] Z. J. Xiao, Y. Y. Fan, W. F. Wang and S. Cheng, "The semileptonic decays of B/B_s meson in the perturbative QCD approach: A short review," Chin. Sci. Bull. **59**, 3787 (2014).

[20] S. J. Brodsky, T. Huang, and G. P. Lepage, in *Particles and Fields-2*, Proceedings of the Banff Summer Institute, Ban8; Alberta, 1981, edited by A. Z. Capri and A. N. Kamal (Plenum, New York, 1983), p. 143; G. P. Lepage, S. J. Brodsky, T. Huang, and P. B.Mackenize, *ibid.* , p. 83;

T. Huang, in *Proceedings ofXXth International Conference on High Energy Physics*, Madison, Wisconsin, 1980, edited by L. Durand and L. G Pondrom, AIP Conf. Proc. No. 69 (AIP, New York, 1981), p. 1000.

[21] T. Zhong, X. G. Wu, Z. G. Wang, T. Huang, H. B. Fu and H. Y. Han, "Revisiting the Pion Leading-Twist Distribution Amplitude within the QCD Background Field Theory", Phys. Rev. D **90**, 016004 (2014).

[22] X. H. Guo and T. Huang, "Hadronic wave functions in D and B decays", Phys. Rev. D **43**, 2931 (1991).

[23] K. A. Olive, et al., (Particle Data Group), "The Review of Particle Physics (2015)", Chin. Phys. C **38**, 090001 (2014).

[24] T. Huang, B. Q. Ma, and Q. X. Shen, "Analysis of the pion wave function in light cone formalism", Phys. Rev. D **49**, 1490 (1994).

[25] G. P. Lepage, S. J. Brodsky, "Exclusive Processes in Perturbative Quantum Chromodynamics", Phys. Rev. D **22**, 2157 (1980).

[26] P. Ball and R. Zwicky, "New results on $B \to \pi, K, \eta$ decay formfactors from light-cone sum rules", Phys. Rev. D **71**, 014015 (2005).

[27] T. Huang, Z. H. Li and X. Y. Wu, "Improved approach to the heavy to light form-factors in the light cone QCD sum rules", Phys. Rev. D **63**, 094001 (2001).

[28] Z. G. Wang, M. Z. Zhou and T. Huang, "B - π weak formfactor with chiral current in the light cone sum rules", Phys. Rev. D **67**, 094006 (2003).

[29] T. Zhong, X. G. Wu, J. W. Zhang, Y. Q. Tang and Z. Y. Fang, "New results on Pionic Twist-3 Distribution Amplitudes within the QCD Sum Rules", Phys. Rev. D **83**, 036002 (2011).

[30] T. Huang, T. Zhong and X. G. Wu, "Determination of the pion distribution amplitude", Phys. Rev. D **88**, 034013 (2013).

[31] Z. H. Li, N. Zhu, X. J. Fan and T. Huang, "Form Factors $f_+^{B\to\pi}(0)$ and $f_+^{D\to\pi}(0)$ in QCD and Determination of $|V_{ub}|$ and $|V_{cd}|$", JHEP **1205**, 160 (2012).

[32] X. G. Wu, T. Huang and Z. Y. Fang, "$SU_f(3)$-symmetry breaking effects of the $B \to K$ transition form-factor in the QCD light-cone sum rules", Phys. Rev. D **77**, 074001 (2008).

[33] X. G. Wu and T. Huang, "Radiative Corrections on the $B \to P$ Form Factors with Chiral Current in the Light-Cone Sum Rules", Phys. Rev. D **79**, 034013 (2009).

[34] T. Huang, Z. H. Li, X. G. Wu and F. Zuo, "Semileptonic $B(B_s, B_c)$ decays in the light-cone QCD sum rules", Int. J. Mod. Phys. A **23**, 3237 (2008).

[35] H. B. Fu, X. G. Wu, Y. Ma, W. Cheng and T. Zhong, "$B \to K^*$ Transition Form Factors and the Semi-leptonic Decay $B \to K^*\mu^+\mu^-$," J. Phys. G **43**, 015002 (2016).

[36] H. B. Fu, X. G. Wu, H. Y. Han and Y. Ma, "$B \to \rho$ transition form factors and the ρ-meson transverse leading-twist distribution amplitude," J. Phys. G **42**, 055002 (2015)

[37] H. B. Fu, X. G. Wu, H. Y. Han, Y. Ma and T. Zhong, "$|V_{cb}|$ from the semileptonic decay $B \to D\ell\bar{\nu}_\ell$ and the properties of the D meson distribution amplitude", Nucl. Phys. B **884**, 172 (2014).

[38] H. Y. Han, X. G. Wu, H. B. Fu, Q. L. Zhang and T. Zhong, "Twist-3 Distribution Amplitudes of Scalar Mesons within the QCD Sum Rules and Its Application to the $B \to S$ Transition Form Factors," Eur. Phys. J. A **49**, 78 (2013).

[39] P. Ball and V. M. Braun, "Exclusive semileptonic and rare B meson decays in QCD," Phys. Rev. D **58**, 094016 (1998).

[40] I. I. Balitsky, V. M. Braun and A. V. Kolesnichenko, "Radiative Decay $\sigma^+ \to p\gamma$ in Quantum Chromodynamics," Nucl. Phys. B **312**, 509 (1989).

[41] V. L. Chernyak and I. R. Zhitnitsky, "B meson exclusive decays into baryons," Nucl. Phys. B **345**, 137 (1990).

[42] V. V. Kiselev, "Exclusive decays and lifetime of B_c meson in QCD sum rules," hep-ph/0211021.

[43] M. A. Ivanov, J. G. Korner and P. Santorelli, "Semileptonic decays of B_c mesons into charmonium states in a relativistic qurk model", Phys. Rev. D **71**, 094006 (2005); Phys. Rev. D **75**, 019901 (2007).

[44] E. Hernandez, J. Nieves and J. M. Verde-Velasco, "Study of exclusive semileptonic and nonleptonic decays of B_c^- in a nonrelativistic quark model", Phys. Rev. D **74**, 074008 (2006).

[45] R. Dhir, R. C. Verma, "B_c Meson Form-factors and $B_c \to PV$ Decays Involving Flavor Dependence of Transverse Quark Momentum", Phys. Rev. D **79**, 034004 (2009).

[46] W. F. Wang, Y. Y. Fan, and Z. J. Xiao, "Semileptonic decays $B_c \to (\eta_c, J/\psi)l\nu$ in the perturbative QCD approach", Chin. Phys. C **3**7, 093102 (2013).

[47] W. Wang, Y. L. Shen, and C. D. Lü, "Covariant Light-Front Approach for B_c transition form factors", Phys. Rev. D **79**, 054012 (2009).

[48] D. Ebert, R. N. Faustov and V. O. Galkin, "Weak decays of the B_c meson to charmonium and D mesons in the relativistic quark model", Phys. Rev. D **68**, 094020 (2003).

[49] J. M. Shen, X. G. Wu, H. H. Ma and S. Q. Wang, "QCD corrections to the B_c to charmonia semileptonic decays", Phys. Rev. D **90**, 034025 (2014).

[50] C. F. Qiao and R. L. Zhu, "Estimation of semileptonic decays of B_c meson to S-wave charmonia with nonrelativistic QCD," Phys. Rev. D **87**, 014009 (2013).

[51] T. Huang and X. G. Wu, "A Model for the twist-3 wave function of the pion and its contribution to the pion form-factor," Phys. Rev. D **70**, 093013 (2004).